

Structure and Topology of Microbial Communities in the Major Gut Compartments of *Melolontha melolontha* Larvae (Coleoptera: Scarabaeidae)

Markus Egert,¹† Ulrich Stingl,^{1,2} Lars Dyrhberg Bruun,¹ Bianca Pommerenke,¹
 Andreas Brune,^{1,2} and Michael W. Friedrich^{1*}

Max Planck Institute for Terrestrial Microbiology, Karl-von-Frisch-Straße, 35043 Marburg, Germany,¹ and
 Fachbereich Biologie, LS Mikrobielle Ökologie, Universität Konstanz,
 78457 Konstanz, Germany²

Received 2 August 2004/Accepted 23 February 2005

Physicochemical gut conditions and the composition and topology of the intestinal microbiota in the major gut compartments of the root-feeding larva of the European cockchafer (*Melolontha melolontha*) were studied. Axial and radial profiles of pH, O₂, H₂, and redox potential were measured with microsensors. Terminal restriction fragment length polymorphism (T-RFLP) analysis of bacterial 16S rRNA genes in midgut samples of individual larvae revealed a simple but variable and probably nonspecific community structure. In contrast, the T-RFLP profiles of the hindgut samples were more diverse but highly similar, especially in the wall fraction, indicating the presence of a gut-specific community involved in digestion. While high acetate concentrations in the midgut and hindgut (34 and 15 mM) corroborated the presence of microbial fermentation in both compartments, methanogenesis was confined to the hindgut. *Methanobrevibacter* spp. were the only methanogens detected and were restricted to this compartment. Bacterial 16S rRNA gene clone libraries of the hindgut were dominated by clones related to the *Clostridiales*. Clones related to the *Actinobacteria*, *Bacillales*, *Lactobacillales*, and γ -*Proteobacteria* were restricted to the lumen, whereas clones related to the β - and δ -*Proteobacteria* were found only on the hindgut wall. Results of PCR-based analyses and fluorescence in situ hybridization of whole cells with group-specific oligonucleotide probes documented that *Desulfovibrio*-related bacteria comprise 10 to 15% of the bacterial community at the hindgut wall. The restriction of the sulfate-reducer-specific adenosine-5'-phosphosulfate reductase gene *apsA* to DNA extracts of the hindgut wall in larvae from four other populations in Europe suggested that sulfate reducers generally colonize this habitat.

Soil macroinvertebrates play an essential role in the cycling of organic matter (55). Numerous coleopteran larvae, particularly those of the Scarabaeidae, feed on fresh or decomposing plant material on or in the soil (13), and many of them are important plant pests. In central Europe, the root-feeding larva of the European cockchafer (*Melolontha melolontha*) causes significant economic damage (28).

In general, the intestinal tracts of many soil insects harbor a dense and diverse microbiota, which functions in the hydrolysis and/or fermentative breakdown of polymeric food components to degradation products that can be resorbed by the host (8, 17, 27). However, only little is known about the contribution of microbial processes to host nutrition (8, 17) and how host factors, such as morphology, compartmentalization, and physicochemical conditions of the intestinal tract, influence the composition and control the activity of the gut microbiota on a microscale (9).

In scarabaeid beetle larvae, the intestinal tract consists of two major compartments: a tubular midgut, which is the site of secretion of numerous hydrolytic enzymes, and a bulbous hind-

gut, which is generally considered a fermentation chamber (24, 41, 53, 54). Although both gut compartments are densely colonized by diverse microorganisms (3, 10), which were recognized early as participating in digestion (52), the composition of the intestinal microbiota and the activities and spatial distribution of microbial populations within the gut have hardly been investigated (reference 10 and references therein).

Only the humivorous larva of *Pachnoda ephippiata* has been characterized in more detail. Like many other insect larvae with a diet rich in tannins and phenols, it is characterized by high midgut alkalinity, which is generally considered to prevent precipitation of dietary proteins and digestive enzymes (21, 36). In *P. ephippiata*, however, the high pH of the midgut fluid seems to be an adaptation to the humivorous lifestyle, rendering the ingested soil organic matter more accessible for microbial degradation (32, 33). Both the midgut and hindgut are characterized by high concentrations of microbial fermentation products and a dense and diverse microbial community that differs clearly between the compartments (20, 32).

However, little is known about the microbiota in scarabaeid larvae from other feeding guilds. Microbiological studies of phytophagous scarabaeid larvae have focused mostly on insect pathogens of several economically important pest species (e.g., *M. melolontha* (28, 29), *Costelytra zealandica* (26), and *Popillia japonica* (30, 39, 44)). Opportunistic pathogens may also be members of the gut microbiota in healthy insects but are not numerically important. Moreover, cultivation-based studies

* Corresponding author. Mailing address: Max Planck Institute for Terrestrial Microbiology, Karl-von-Frisch-Straße, 35043 Marburg, Germany. Phone: 49-6421-178830. Fax: 49-6421-178809. E-mail: michael.friedrich@staff.uni-marburg.de.

† Present address: Laboratory of Microbiology, Wageningen University, Hesselink van Suchtelenweg 4, 6703 CT Wageningen, The Netherlands.

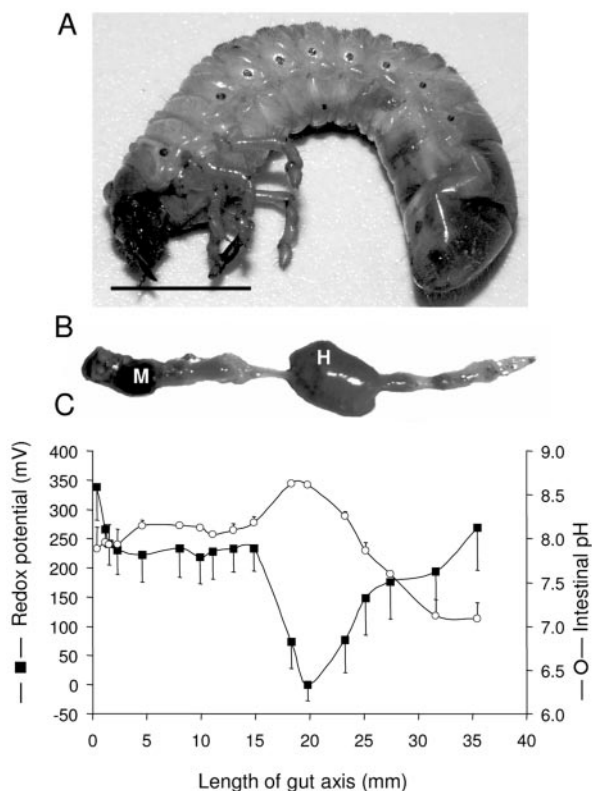


FIG. 1. Habitus (A) and excised gut (B) of an *M. melolontha* larva (late second larval instar). M, midgut; H, hindgut; the scale bar represents ca. 1 cm. (C) Profiles of redox potential and intestinal pH along the axis of intact guts incubated in aerated Ringer's solution. Each value represents the mean \pm SEM of three replicate guts.

are usually unable to give an unbiased view of community structure in any ecosystem (2).

In contrast to numerous studies of termites (for a review, see reference 8), a cultivation-independent characterization of the intestinal microbial community of coleopteran species has been conducted only with the humivorous larva of *P. ephippiata* (20). Here, we report on the prokaryotic community in the gut of the phytophagous larva of *Melolontha melonthea*. The study entailed a microsensors analysis of the physicochemical conditions in the intestinal tract and an analysis of the structure and topological organization of the microbial community using a combination of several molecular techniques.

MATERIALS AND METHODS

Insects and gut preparation. Late second and third larval instars of the European cockchafer (*M. melolontha* L.) (Fig. 1A) were collected in 2002 and 2003 near Obergrombach, Germany (for the origins of all other larvae, see Table 4). Until analysis, the larvae were kept separately in meadow soil at 15°C for up to several months and fed with grass roots, and only actively feeding insects were used for the experiments. Larvae were dissected as described previously (32), and the gut compartments were separated at the midgut-hindgut junction (Fig. 1B). For preparation of wall and lumen fractions, the gut compartments were opened with scissors and the gut content was removed with a sterile spatula. Subsequently, the gut walls were washed three times with sterile Ringer's solution.

Microsensor measurements. Oxygen, hydrogen, pH, and redox potentials were measured with microsensors in freshly dissected guts irrigated with Ringer's solution as previously described in detail (11).

Metabolites in gut fluids and hemolymph. Hemolymph, collected via an incision in the integument before the larvae were decapitated, and gut sections were

treated as follows: mild sonification, centrifugation (14,000 \times g; 10 min), addition of 5 μ l H₂SO₄ (5 M) per 95 μ l supernatant, centrifugation (14,000 \times g; 10 min), and measurement of the supernatant (50 μ l) for metabolites (i.e., glucose, organic acids, and alcohols) by high-pressure liquid chromatography (49). For sulfate determination, supernatants (~50 μ l) were diluted twofold with HCl (0.5 M), centrifuged (10 min; 10,000 \times g) again, and analyzed using ion chromatography.

Methane production rates. The methane production rates of larvae and isolated gut sections were determined as previously described in detail (32). Stimulation of methane emission was tested by supplementing the headspace with H₂ (5%; larvae and gut sections) or by adding Na formate (5 mM; gut sections only) after the basal rate of methane production had been established.

DNA extraction and PCR amplification of 16S rRNA and *apsA* genes. DNA was extracted and purified from gut samples and food plant roots as previously described (20). 16S rRNA genes were amplified using primers 27f and 907r (37) or Ar109f and Ar915r for bacterial and archaeal clone libraries, as described elsewhere in detail (19, 20). The *apsA* gene encoding the α subunit of the adenosine-5'-phosphosulfate (APS) reductase of sulfate-reducing bacteria (SRB) was amplified with the primers APS7-F and APS8-R as described elsewhere (22), except that 1 μ l of a 1:20 dilution of DNA extract was added as a template and a thermal PCR profile with 35 cycles at an annealing temperature of 52°C was used.

16S rRNA gene libraries and analysis of sequence data. Bacterial and archaeal 16S rRNA gene amplicons were cloned in *Escherichia coli* as described previously (20). Bacterial clones retrieved from DNA extracts of the hindgut lumen and hindgut wall of an individual larva were designated MKEL and MKEW, respectively. Archaeal clones obtained from a DNA extract of a complete hindgut were named MKED. Sequence data were analyzed and trees were constructed using the ARB software package with its database (version 2.5b; O. Strunk and W. Ludwig, Technische Universität München, München, Germany [http://www.arb-home.de]) as described elsewhere (20).

T-RFLP analysis. Terminal restriction fragment length polymorphism (T-RFLP) analysis was performed as described elsewhere (20). Briefly, 16S rRNA genes were specifically amplified using the combinations 6-carboxyfluorescein-labeled primer 27f and primer 907r for *Bacteria* and primer Ar109f and 6-carboxyfluorescein-labeled primer Ar915r for *Archaea*. DNA was restricted with *MspI* for bacterial amplicons and *AluI* for archaeal amplicons. Terminal restriction fragments (T-RFs) in the profiles were assigned to phylotypes based on in silico analysis of the clones in the respective libraries. In addition, all clones were checked in vitro for the formation of pseudo-T-RFs, and pseudo-T-RFs in profiles of gut samples were identified by mung bean nuclease treatment prior to endonuclease restriction (18).

Total cell counts and fluorescence in situ hybridization (FISH). Homogenized, phosphate-buffered-saline-diluted gut samples were fixed overnight with paraformaldehyde (3% [wt/vol]) (PFA) at 4°C or ethanol (50% [vol/vol]) at -20°C, transferred onto white polycarbonate membrane filters (0.2 μ m GTTP; Millipore, Eschborn, Germany), washed with phosphate-buffered saline (only PFA-fixed samples), air dried, and stored at -20°C. Samples were dehydrated with an ethanol series, hybridized with CY-3-labeled oligonucleotide probes (35% formamide in hybridization buffer), washed, and counterstained with 4,6-diamino-2-phenylindole (DAPI) as described previously (38). The filters were embedded in Citifluor solution (AF1; Citifluor Ltd., London, United Kingdom), and the cells (\geq 1,000 per sample) were counted with an epifluorescence microscope.

Estimation of ecological indices and statistical analyses. The bacterial species richness of the hindgut lumen and hindgut wall was calculated using Chao1 as a nonparametric estimator (20). T-RFLP profiles were normalized, and the diversity (Shannon-Wiener index), evenness, and community similarity (Morisita) indices were calculated as described elsewhere (19). Differences between samples (in ecological indices, physicochemical parameters, or FISH cell counts) were checked for statistical significance ($P \leq 0.05$) with nonparametric Mann-Whitney tests using SYSTAT 10.0 (SPSS Inc., Chicago, Ill.).

Nucleotide sequence accession numbers. The bacterial 16S rRNA gene sequences of MKEL and MKEW clones are accessible under accession numbers AJ852243 to AJ852332 and AJ852333 to AJ852406, respectively. Three representative archaeal sequences (MKED clones) are accessible under AJ852240 to -42.

RESULTS

Microsensor measurements. The intestinal tracts of *M. melolontha* larvae (Fig. 1B) were characterized by only mod-

TABLE 1. Concentration of metabolites in major gut compartments and hemolymph of *M. melolontha* larvae

Metabolite ^a	Concn (mM) ^b		
	Midgut	Hindgut	Hemolymph
Acetate	33.6 ± 6.3 a	14.8 ± 3.4 b	3.2 ± 1.2 c
Lactate	1.8 ± 0.1 a	0.4 ± 0.2 a	1.4 ± 0.5 a
Propionate	– a ^c	0.2 ± 0.2 a	– a ^c
Succinate	0.8 ± 0.2 a	0.2 ± 0.1 b	2.9 ± 0.9 a
Glucose	12.0 ± 4.2 a	0.9 ± 0.4 b	2.9 ± 0.9 b

^a Not detected (detection limit in parentheses): ethanol (0.4 mM), formate (0.3 mM), butyrate (0.15 mM), isobutyrate (0.10 mM), isovalerate (0.1 mM).

^b Values are mean ± standard error of the mean ($n = 4$). Means within rows followed by the same letter are not significantly ($P < 0.05$) different.

^c Below detection limit (0.15 mM).

erate dynamics of the pH and larger dynamics of the redox potential. The pH was rather constant in the midgut (pH 7.9 to 8.2) and decreased along the hindgut from slightly alkaline (pH 8.6) in the hindgut paunch to neutral conditions in the colon and rectum (Fig. 1C). The redox potential (E_h) in the midgut ranged from +220 to +340 mV (Fig. 1C), indicating that oxidizing conditions dropped sharply at the midgut-hindgut junction, attained a minimum (0 mV) in the anterior hindgut, and increased again toward the rectum. Radial profiles of oxygen concentrations in both gut compartments revealed steep gradients of O₂ over the gut wall penetrating less than 100 μm into the lumen, indicating largely anoxic conditions in the midgut and hindgut (details not shown). Axial hydrogen concentration profiles showed only a slight accumulation of H₂ (0.3 to 1.1 kPa) restricted to the central part of the midgut (details not shown).

Methane production rates. The methane emission rates of individual larvae were stimulated twofold by the addition of H₂ to the headspace (from 51 ± 9 to 96 ± 7 nmol g [fresh wt.]⁻¹ h⁻¹; $n = 5$). Incubation of isolated gut compartments under an N₂ atmosphere revealed that CH₄ emission was restricted to the hindgut (23 ± 10 nmol g [fresh wt.]⁻¹ h⁻¹; $n = 3$), corresponding to approximately half of the rate observed with living animals. CH₄ emission rates of isolated hindguts were almost identical when the guts were incubated under air or in the presence of formate but increased twofold under H₂.

Microbial fermentation products and sulfate. Both gut compartments contained short-chain fatty acids and other metabolites typical of microbial fermentations, in particular acetate (Table 1). The concentrations of acetate and succinate were significantly higher in the midgut than in the hindgut. The spectrum of metabolites in the hemolymph resembled that in the gut compartments, although the concentrations, in particular that of acetate, were considerably lower than in the gut. Also, glucose accumulated to relatively high concentrations in all compartments, particularly in the midgut. The sulfate concentration was significantly higher in the midgut than in the hindgut (2.9 ± 0.6 and 0.9 ± 0.3 mM; $n = 5$).

Microbial diversity in different gut habitats. The bacterial diversity in the wall and lumen fractions of the two major gut compartments of three different larvae was analyzed by T-RFLP fingerprinting of 16S rRNA genes and compared to the pattern obtained for the larval diet (plant roots) (Fig. 2). While the hindgut profiles of all larvae consistently displayed a high

number of T-RFs, the midgut profiles of two larvae showed only one or three major T-RFs, with a prominent peak at 495 bp. This T-RF, however, was missing in a third larva (Fig. 2). The low diversity of the bacterial community in the midgut samples contrasted sharply with the high diversity of the root samples (Fig. 2).

By contrast, the profiles of the hindgut wall fractions were very similar to each other. Morisita indices of community similarity between the individual hindgut wall profiles were significantly higher than that of the lumen profiles (89 ± 3% versus 68 ± 1%) and were significantly higher than the average similarity between the hindgut wall and lumen profiles derived from the same individual (72 ± 5%). However, the ecological indices of community diversity (Shannon-Wiener; 2.78 ± 0.02 versus 2.88 ± 0.10) and evenness (0.93 ± 0.01 versus 0.93 ± 0.02) of the two fractions were very similar. Ecological indices were not calculated for the midgut because of the large individual differences in the T-RFLP profiles and lack of consistency between the larvae.

While no archaeal 16S rRNA genes could be amplified from midgut samples, T-RFLP profiles of all wall and lumen fractions uniformly displayed a dominant 67-bp T-RF (and a smaller 167-bp pseudo-T-RF), which could be assigned to *Methanobrevibacter*-related clones (data not shown).

16S rRNA gene clone libraries. Two separate bacterial clone libraries were generated from DNA extracts of the lumen and wall fraction of an individual hindgut; a third (archaeal) clone library was generated from the complete hindgut of another larva. From all clone libraries, randomly selected clones were sequenced and phylogenetically analyzed. All clones were affiliated with established major lines of descent among the *Bacteria* (Fig. 3, 4, and 5 and Table 2) and the *Archaea* (not shown). Within each lineage, many of the clones from this study clustered with cultured representatives and/or clones from the intestinal tracts of other insects (particularly termites and cetoniid beetle larvae) or higher animals (ruminants, rodents, pigs, and humans).

Bacterial clones obtained from the hindgut lumen ($n = 90$) were assigned to seven distinct phylogenetic groups (Fig. 3 to 5). Most lumen clones (47%) were affiliated with the *Clostridiales* (Fig. 3). Several of them could be assigned to the clostridial clusters IV, IX, XIVa and b, and XVI sensu Collins et al. (12); however, many grouped (together with other intestinal clones or isolates) outside of these clusters. Twenty-four lumen clones clustered with *Turicibacter sanguinis* (92 to 97% sequence identity), a strictly anaerobic, gram-positive bacterium isolated from a human blood sample (5). Members of the *Actinobacteria*, *Bacillales*, *Lactobacillales*, γ -*Proteobacteria*, and *Bacteroidetes* were less frequently recovered; with the exception of the *Bacteroidetes*, these clones were found exclusively in the clone library of the hindgut lumen (Fig. 4 and 5).

The 74 bacterial clones from the hindgut wall sample fell into five distinct phylogenetic groups (Fig. 3 to 5). Most clones of the gut wall (61%) were affiliated with the *Clostridiales* and grouped within clostridial clusters I, IV, XI, and XIVa or outside of known clusters (Fig. 3). Twelve clones derived from the gut wall were related to members of the *Bacteroidetes*, but none of them clustered with the genus *Dysgonomonas*; such clones were present exclusively in the library of the lumen fraction (Fig. 4). The most prominent difference between the

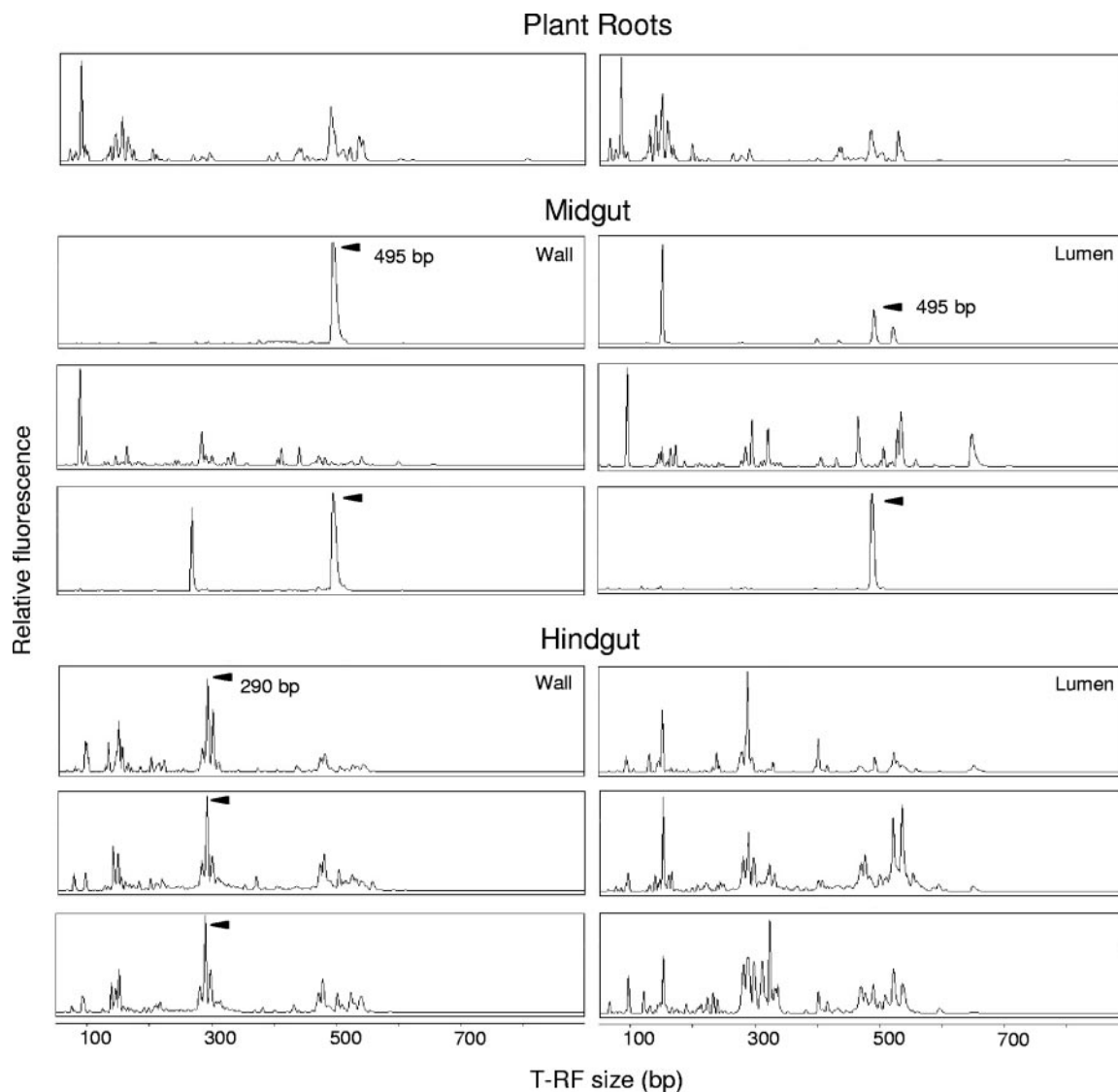


FIG. 2. Bacterial 16S rRNA gene T-RFLP profiles obtained from DNA extracts of three individual *M. melolontha* larvae and from two food samples (roots with attached soil). The excised guts were separated into compartments (midguts and hindguts) and each compartment into two subcompartmental fractions (gut wall and lumen). Prominent peaks referred to in the text are indicated. *MspI* was used for restriction digestion.

two clone libraries, however, was the distribution of the δ -proteobacterial clones, which were all affiliated with the genus *Desulfovibrio* and comprised 15% of all clones derived from the hindgut wall but were completely absent from the lumen library (Fig. 5 and Table 2). The closest relative was *Desulfovibrio cuneatus* (85.6 to 88.5% sequence identity), isolated from an oxic freshwater sediment (42).

By using an arbitrarily defined limit of 97% sequence identity (45), the 16S rRNA gene clones in the hindgut lumen and wall libraries were grouped into 39 and 45 different phylotypes, respectively. Using Chao1 as a nonparametric richness estimator, the estimated total numbers of phylotypes were 63 for the hindgut lumen and 127 for the wall, which indicates that cloning analysis detected 62% and 35% of the phylotypes present in the respective fractions.

All 30 archaeal clones were virtually identical (>99.8% sequence identity) and clustered within the *Methanobacteriaceae*

(details not shown); they were closely related to *Methanobrevibacter arboriphilus* (AB065294; ~97.8% sequence identity) and to clones from the intestinal tracts of humivorous *P. ephippiata* beetle larvae (AJ576150 and AJ576127; ~99.5% sequence identity) (20).

T-RFLP analysis of 16S rRNA gene frequency. All phylogenetic groups in the clone libraries of the hindgut wall and lumen were represented by T-RFs in the respective T-RFLP profiles; taken together, the assigned T-RFs accounted for ~81% of the total peak height in both profiles (Fig. 6). In general, T-RFLP-based gene frequencies corroborated the clone frequencies in the clone libraries (Table 2); any differences were most likely caused by the fact that clone frequencies are generally biased by undersampling (51).

In the cases of both the hindgut wall and lumen, the most prominent peak in the respective T-RFLP profile represented a T-RF of 290 bp. In the lumen clone library, all clones with

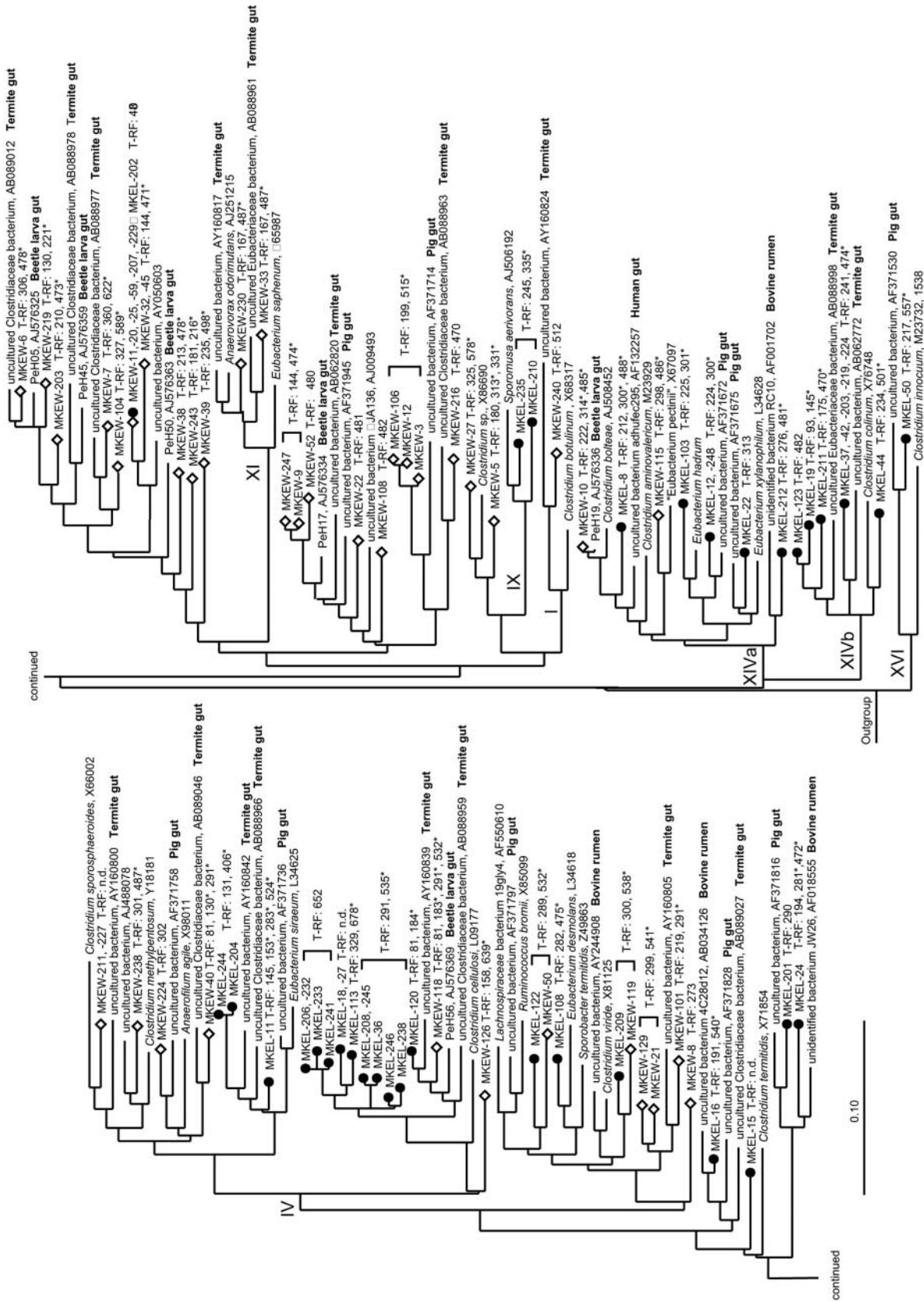


FIG. 3. Phylogenetic tree showing the positions of 16S rRNA gene sequences affiliated with the *Clostridiales* recovered from the hindgut lumen (filled circles) and the hindgut wall (open diamonds) of an *M. melolontha* larva. For tree construction with distance matrix-based neighbor joining, 667 sequence positions (*Escherichia coli* positions 64 to 877) were used. The scale bar represents 10% sequence difference. Accession numbers of reference sequences are indicated. Species used as outgroups were *Thermus thermophilus* (M26923), *Feridobacterium gondwanense* (Z4917), and *Thermotoga maritima* (M21774). The Roman numerals indicate clostridial subgroups sensu Collins et al. (12). The lengths of T-RFs result from in vitro digestion of clonal 16S rRNA gene amplicons with MspI; pseudo-T-RFs (18) are marked with asterisks. n.d., T-RF length not determinable.

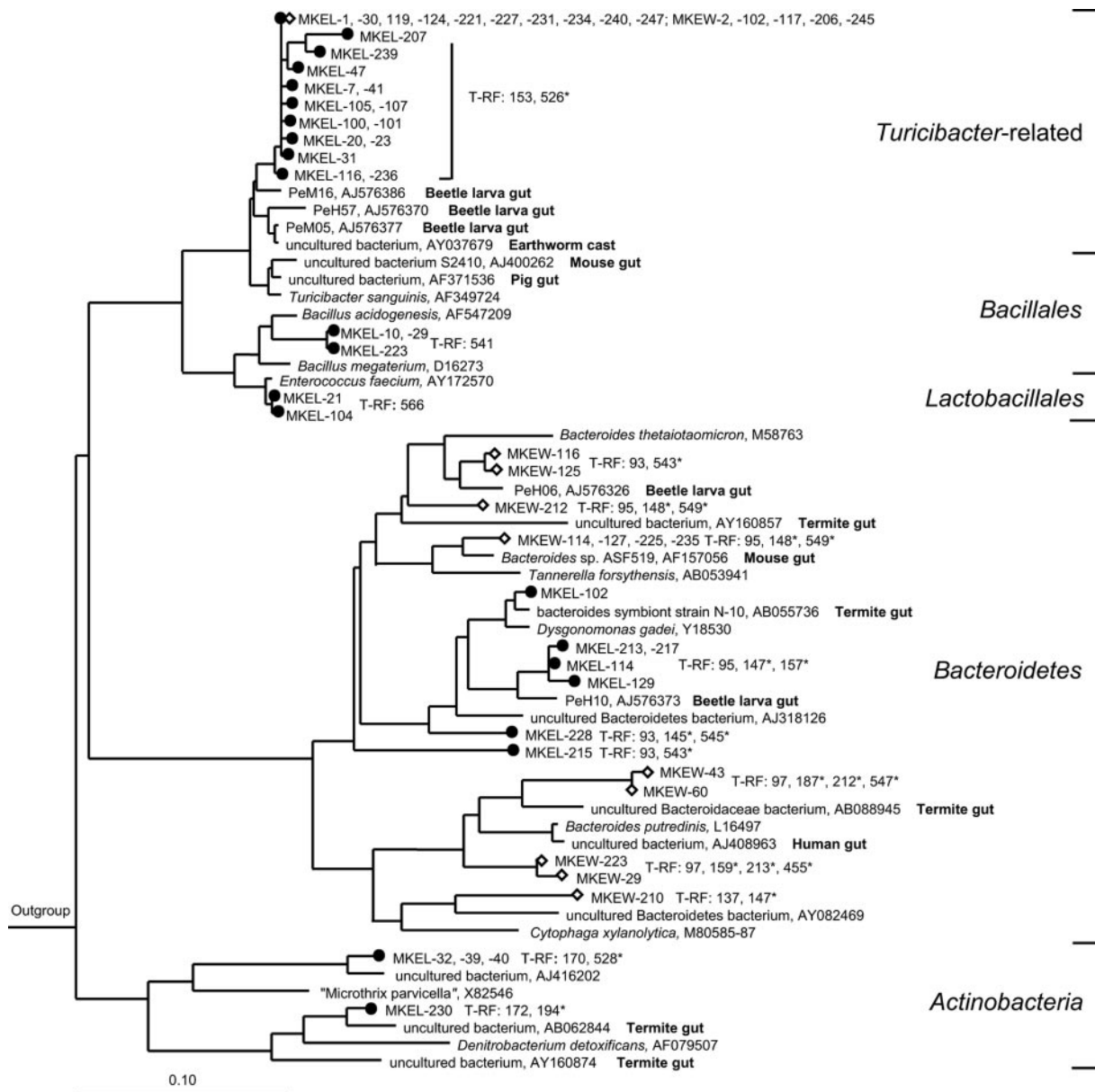


FIG. 4. Phylogenetic tree showing the positions of 16S rRNA gene sequences affiliated with *Turicibacter* spp., *Bacillales*, *Lactobacillales*, *Bacteroidetes*, and *Actinobacteria* recovered from the hindgut lumen (filled circles) and the hindgut wall (open diamonds) of an *M. melolontha* larva. The scale bars represent 10% sequence difference. For additional information (nucleotide positions used, treeing method, outgroup, and T-RFs), see the legend to Fig. 3.

this T-RF length are affiliated with the *Clostridiales*. By contrast, almost all clones in the wall clone library fall within the genus *Desulfovibrio*, and only one clone (MKEW-50) is affiliated with the *Clostridiales*, indicating that the 290-bp peak in the hindgut wall sample largely represents *Desulfovibrio* species. In this case, the relative gene frequency of *Desulfovibrio* spp. would be close to 15%, which agrees well with the corresponding clone frequency (Table 2). Also in the hindgut wall profiles of the two other larvae, the 290-bp T-RF represents 12 to 15% of the total peak height (Fig. 2).

Cell densities and FISH analysis. Total cell counts in the midgut compartment were approximately fivefold lower than

in the hindgut (Table 3). The proportion of DAPI-stained cells hybridizing with a mixture of oligonucleotide probes targeting all *Bacteria* was relatively low in the midgut but considerably higher in the hindgut. However, only the hindgut homogenates contained a small proportion of cells hybridizing with probes targeting all *Archaea*. Notably, archaeal cells were detected only after fixation with ethanol, but not with PFA.

The spatial distributions of microorganisms in the hindgut were studied in lumen and wall fractions of individual larvae (Table 3). Based on DAPI counts and fresh weight, cell density at the hindgut wall was approximately 3.5-fold higher than that in the hindgut lumen. The fraction of DAPI-stained cells that

TABLE 2. Relative abundances of major phylogenetic groups in the hindgut lumen and on the hindgut wall of an *M. melolontha* larva^a

Phylogenetic group	Abundance (%)			
	Hindgut lumen		Hindgut wall	
	Clone library	T-RFLP	Clone library	T-RFLP
<i>Actinobacteria</i>	4.4	1.0	— ^b	—
<i>Bacillales</i>	3.3	1.4	—	—
<i>Lactobacillales</i>	2.2	0.7	—	—
<i>Turicibacter</i> related	26.7	15.3	6.8	1.0–4.9
<i>Clostridiales</i>	46.7	58.9–60.1	60.8	38.1–52.5
<i>Bacteroidetes</i>	7.8	3.1–4.3	16.2	22.3
β - <i>Proteobacteria</i>	—	—	1.4	0–3.9
γ - <i>Proteobacteria</i>	8.9	2.8	—	—
δ - <i>Proteobacteria</i>	—	—	14.9	0.8–15.3

^a Based on the frequencies of 16S rRNA genes in clone libraries ($n = 90$ [lumen] and 74 [wall]) and on T-RFLP analysis. Since some T-RFs were shared by more than one phylogenetic group (Fig. 6), the T-RFLP-based frequencies of these groups can be expressed only as frequency ranges. Minimum frequencies were calculated by considering only those T-RFs that were unique to a certain group, whereas for maximum frequencies, those T-RFs shared with others were also taken into account.

^b —, not detected.

hybridized with the *Bacteria*-specific EUB 338 probes (Table 3) was not significantly different between the lumen and wall fractions. Most of the archaeal cells were located at the hindgut wall.

Probe SRB385, which generally targets sulfate-reducing bacteria affiliated with the δ -*Proteobacteria*, had one mismatch to all *Desulfovibrio*-related clones in the hindgut wall clone library, located at the 5' end of the target sequence, and also only one mismatch to clones of certain gram-positive bacteria, albeit at the center of the target sequence. Therefore, we also counted sulfate-reducing bacteria with the newly designed probe DSV698-MK, which matched exactly 10 of the 11 *Desulfovibrio*-related sequences obtained in this study and had at

least two mismatches to all other clones in the hindgut clone libraries.

Despite the differences in specificity, the results obtained with probe DSV698-MK and with probe SRB385 were virtually identical, indicating that 9 to 10% of all bacterial cells colonizing the hindgut wall were *Desulfovibrio* spp., which is in agreement with the clone frequency in the clone library of the hindgut wall and corroborated our interpretation of the T-RFLP profiles (see above).

Sulfate-reducing bacteria in larvae of different geographic origins. The presence of *Desulfovibrio* spp. on the hindgut walls of *M. melolontha* larvae was determined for four other populations of larvae of different geographic origins (Table 4). Although these larvae had been kept in a sphagnum substrate at $\sim 15^\circ\text{C}$ and had been fed with carrots instead of grass roots, all T-RFLP profiles of hindgut lumen and hindgut wall fractions showed the T-RF of 290 bp, present with similar peak height also in the profiles of the Obergrombach larvae. However, only the DNA from the hindgut wall fraction yielded a PCR product with primers specifically targeting the functional marker gene *apsA* of sulfate-reducing bacteria (Table 4), indicating that *Desulfovibrio* spp. form a significant proportion of the bacteria colonizing the hindgut walls of all *M. melolontha* larvae, irrespective of origin and diet.

DISCUSSION

With the exception of a recent study of termites (56), the topological organization of the intestinal microbiota within individual gut compartments of arthropods has not been studied. In this study of *M. melolontha* larvae, we show that there are axial differences in the community structure, similar to the situation in the humus-feeding larva of *P. ehippiata* (20), probably reflecting the different physicochemical conditions in the respective gut compartments. Moreover, we found significant differences in the bacterial colonization of the lumen and wall fractions of the hindgut, documenting that the microbial

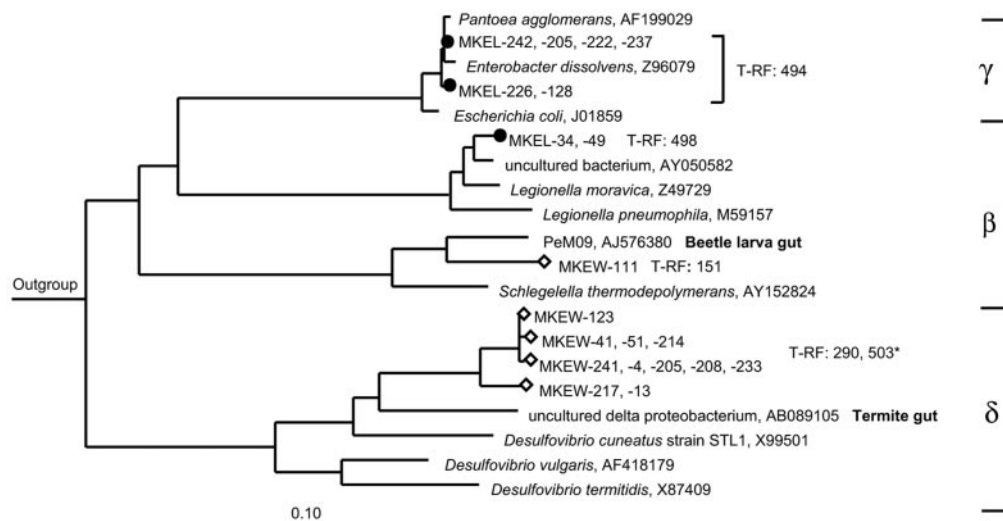


FIG. 5. Phylogenetic tree showing the positions of 16S rRNA gene sequences affiliated with members of the *Proteobacteria* recovered from the hindgut lumen (filled circles) and the hindgut wall (open diamonds) of an *M. melolontha* larva. The scale bars represent 10% sequence difference. For additional information (nucleotide positions used, treeing method, outgroup, and T-RFs), see the legend to Fig. 3.

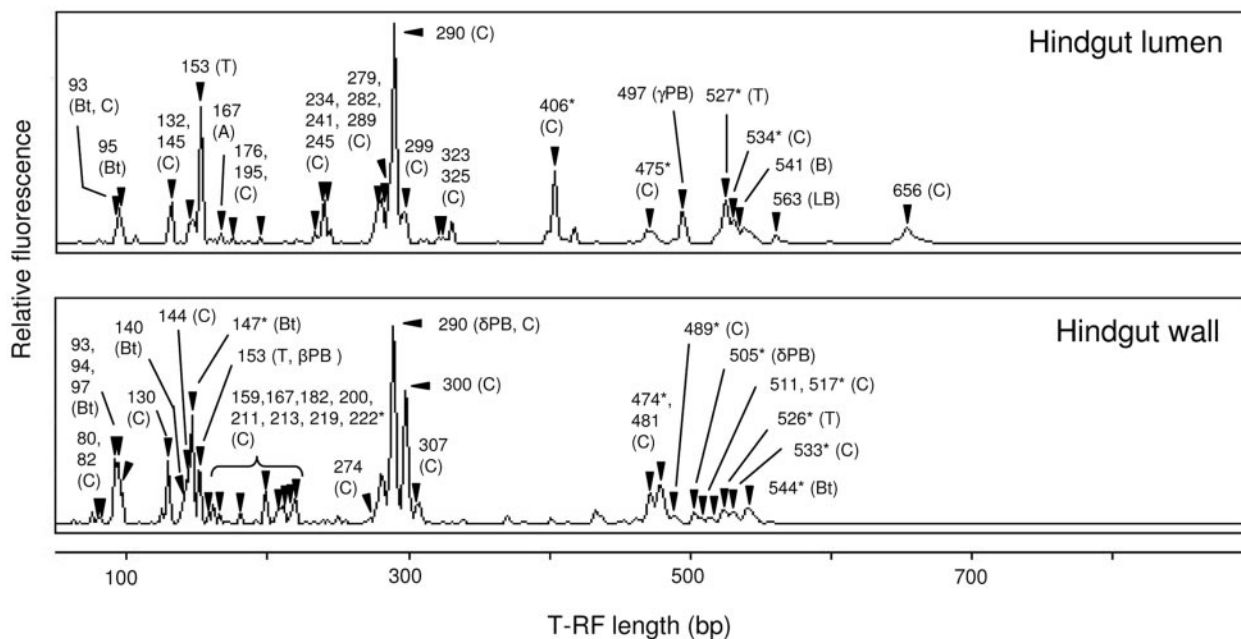


FIG. 6. T-RFLP profiles of bacterial 16S rRNA genes amplified from a hindgut lumen and a hindgut wall sample of an *M. melolontha* larva. MspI was used for restriction digestion. Assignable T-RFs are marked with triangles. Asterisks indicate T-RFs probably influenced by pseudo-T-RF formation (18). Assignable groups are given in parentheses with the following abbreviations: A, *Actinobacteria*; B, *Bacillales*; Bt, *Bacteroidetes*; C, *Clostridiales*; LB, *Lactobacillales*; βPB, β-*Proteobacteria*; δPB, δ-*Proteobacteria*; γPB, γ-*Proteobacteria*; T, *Turicibacter* related.

community is also structured on the radial scale. The abundant population of sulfate-reducing bacteria restricted to the hindgut wall indicates that the topology of the microbiota has important functional implications.

Axial differences in community structure. In scarab beetle larvae, differences between midgut and hindgut communities have already been documented for the humivorous larva of *Pachnoda ephippiata* (20). However, the larva of *P. ephippiata* possesses a highly alkaline midgut (pH > 10), whereas the hindgut is only slightly alkaline (pH 8.5) (32), similar to the phytophagous and humivorous larvae of other Scarabaeidae (for references, see reference 32), and intestinal pH is considered an important determinant of community structure (20,

43). In *M. melolontha* larvae, however, the pH of the midgut is almost identical to that of the slightly alkaline hindgut (Fig. 1C), so that other parameters must be responsible for the differences in microbial colonization.

From a microbial viewpoint, the midgut and hindgut of *M. melolontha* are fundamentally different habitats. As in all insects (47), the midgut of scarab beetle larvae is the site of secretion of numerous digestive enzymes of host origin, which provide easily degradable substrates for the microbiota (for references, see reference 33). Moreover, the passage of the food through the midgut is considerably faster than in the hindgut. In *M. melolontha* larvae, the intestinal transit time is 4 to 8 h in the midgut and up to 4 days in the hindgut (54). As

TABLE 3. Abundances of microorganisms in different gut fractions of *M. melolontha* larvae^a

Compartment	DAPI count (10 ⁹ cells g ⁻¹) ^b	FISH count			
		Domain specific (% DAPI counts)		Group specific (% EUB counts)	
		EUB ^c	ARC ^d	SRB385 ^e	DSV698-MK ^f
Midgut	3.2 ± 1.2	36–47	ND ^g		
Hindgut	15 ± 6	62–74	0.1–0.2		
Wall fraction	32 ± 7	54 ± 5	0.7 ± 0.1	9.4 ± 1.9	8.7 ± 2.0
Lumen fraction	9.5 ± 3.7	60 ± 3	0.1 ± 0.1	0.7 ± 0.1	1.1 ± 0.9

^a Based on DAPI counts and on FISH with group-specific oligonucleotide probes. The values are means ± standard errors of the mean for gut compartments (n = 5) or hindgut fractions (n = 3) of individual larvae; only ranges are given for FISH counts in the midgut and hindgut (n = 2). With the exception of the EUB counts, the differences between gut compartments or between hindgut fractions are significantly different (P < 0.05).

^b Based on fresh weight.

^c Equimolar mixture of probes EUB338, EUB338 II, and EUB338 III, specific for members of the domain *Bacteria* (15).

^d Equimolar mixture of the probes ARC344 (40) and ARCH915 (46), specific for members of the domain *Archaea*.

^e Probe SRB385 (1).

^f Probe DSV698-MK (5'-GTT-CCT-CCT-GAT-CTC-TAC-GG-3'; this study) is based on probe DSV698 (35); modified residues are in boldface.

^g ND, not detected.

TABLE 4. Relative frequencies (based on total profile peak height) of 290-bp T-RFs in bacterial 16S rRNA gene profiles obtained from DNA extracts of hindgut lumen and hindgut wall of *M. melolontha* larvae from different populations and results of PCRs targeting the APS-reductase gene *apsA* in the same DNA extracts

Origin of larvae	Larva	Hindgut lumen		Hindgut wall	
		290-bp T-RF (%)	<i>apsA</i> PCR	290-bp T-RF (%)	<i>apsA</i> PCR
Switzerland ^a	1	3.8	–	13.5	+
	2	3.3	–	8.2	+
Italy ^b	1	22.2	–	16.6	+
	2	14.2	–	18.7	+
Germany ^c	1	3.5	–	21.0	+
	2	6.8	–	14.3	+
Denmark ^d	1	6.4	–	7.2	+

^a Meadow near Lungern, Oberwalden, Switzerland.

^b From Schlanders, South Tyrolia, Italy.

^c Vineyard near Endingen-Kiechlinsbergen, Baden-Württemberg, Germany.

^d Fir plantation near Hadsund, Northern Jylland, Denmark.

in other scarab beetle larvae (references 25 and 32 and references therein), the hindgut of *M. melolontha* larvae has a consistently lower redox potential than the midgut and is the exclusive site of methanogenesis. However, the low rates of methane emission by the larvae suggest that methanogenesis is apparently not an important process in the hindgut of *M. melolontha* larvae, which is in agreement with the low number of *Archaea* determined by FISH.

Compartmental specificity. In the herbivorous caterpillar of the gypsy moth, bacterial community compositions in the midgut were similar among individuals feeding on the same plant leaves but changed dramatically when larvae were shifted to another diet (6). In *M. melolontha*, the midgut community structure varied even among individuals feeding on the same diet, suggesting a rather variable composition of the midgut microbiota. In most larvae, the bacterial diversity in the midgut was reduced compared to the high diversity present in the diet (Fig. 2), indicating lysis of dietary microorganisms in the midgut.

The bacterial community structure in the hindgut, however, was much more diverse than that in the midgut. Especially in the case of the hindgut wall fraction, T-RFLP profiles were highly similar among all individuals investigated, providing a strong argument for an autochthonous, possibly host-specific community with an important role in the intestinal processes. This is supported by the close phylogenetic relationships of the clones in the hindgut clone libraries with clones or isolates retrieved from other intestinal habitats.

Functional implications. The high acetate concentrations in the midgut and hindgut of *M. melolontha* larvae are indicative of an actively fermenting microbiota in both compartments. Nevertheless, the strong accumulation of glucose in the midgut documents that the rate of hydrolysis of plant polymers exceeds the rate of microbial fermentation, allowing glucose absorption by the midgut epithelium. The glucose concentration in the hindgut is considerably lower, caused by either higher fermentation rates or lower rates of hydrolysis of the more recalcitrant residues (e.g., cellulose). This is corroborated by higher cell densities in the hindgut, and a large proportion of clones in the hindgut clone libraries were related to bacterial

taxa with fermentative and often polymer-degrading representatives, such as the *Clostridiales* and *Bacteroidetes*. The presence of microbial fermentation products in the hemolymph suggests that, as in other insects, fermentation products of the gut microbiota are resorbed by the host (7). The high proportion of acetate among the fermentation products in the gut fluid is interesting, since the closest relatives of many hindgut clones (e.g., in the genera *Clostridium*, *Bacteroides*, and *Dysgonomonas*) also form other fermentation products in pure culture. In view of the low hydrogen partial pressure and the low rates of methanogenesis, this may indicate that many of the hindgut clones represent homoacetogenic bacteria.

In contrast to humivorous *P. ephippiata* larvae (32), the lactate concentration in the *M. melolontha* hindgut was almost negligible. Clones related to the *Lactobacillales* were detected only at low frequency, but 18% of all clones in the hindgut clone libraries were closely related to the lactate-producing *Turicibacter sanguinis* (5). Therefore, low lactate concentrations might also be explained by a high rate of lactate turnover, as in the case of the termite *Reticulitermes flavipes* (48).

Radial organization. Microscopic observation revealed that the hindgut wall is covered by a thick biofilm of microorganisms that colonize the treelike chitin structures characteristic of the hindguts of scarabaeid beetle larvae (25), while the rest of the hindgut microbiota is either freely suspended in the gut fluid or attached to the root pieces abundant in the hindgut lumen (M. Egert, L. Dyhrberg-Bruun, and M. W. Friedrich, unpublished results). Differences between the clone libraries of the wall and lumen fractions indicate that the *Actinobacteria*, *Bacillales*, *Lactobacillales*, and γ -*Proteobacteria* are located exclusively in the hindgut lumen, whereas the *Bacteroidetes* are also present on the hindgut wall. However, all *Bacteroidetes* clones from the lumen were closely related to the genus *Dysgonomonas*, whereas the clones from the wall biofilm clustered with *Bacteroides* and *Cytophaga* species. Also, the clostridial clones usually clustered with clones from the same hindgut fraction (Fig. 3), reflecting a pronounced radial organization of the hindgut community. It is suggestive to assume that washout of unattached microorganisms and microoxic conditions in the gut periphery are important determinants of community structure.

Sulfate-reducing bacteria. The most prominent group of microorganisms located almost exclusively in the gut periphery was affiliated with the genus *Desulfovibrio*. They seem to be present in all larvae from geographically different populations and represent 10 to 15% of the bacteria colonizing the hindgut wall. *Desulfovibrio* species are also found in termite guts (23, 50) and in the gastrointestinal tracts of higher animals (16, 34). Berchtold and coworkers (4) have localized sulfate reducers on the hindgut wall of the termite *Mastotermes darwiniensis* by FISH; cells hybridizing with probe SRB385 amounted to approximately 7% of the EUB counts, which is in the same range as the value obtained for *M. melolontha* with probe DSV698-MK (this study).

The high abundance of *Desulfovibrio* spp. on the hindgut wall of *M. melolontha* suggests an important physiological role in hindgut metabolism. The gut fluid of *M. melolontha* contains appreciable concentrations of sulfate (this study), and sulfate has also been detected in the guts of termites and cockroaches (31). The source of intestinal sulfate in *M. melolontha* is un-

known, but in view of the large number of *Desulfovibrio*-related bacteria in the hindgut, the decrease in the sulfate concentration between the midgut and hindgut might be caused by the activity of sulfate-reducing bacteria.

Many sulfate-reducing bacteria, including *Desulfovibrio* spp., respire oxygen even in the presence of sulfate (14), and the termite gut isolate *Desulfovibrio termitidis* has the highest oxygen respiration rate of all prokaryotes investigated (31). The thick biofilm in the hindgut periphery of *M. melolontha* should be at least partially oxic, and it is possible that sulfate-reducing bacteria participate in oxygen removal in the hindgut periphery. However, this depends on their position relative to the oxygen gradient in the biofilm.

Conclusions. Resolving the spatial distribution of microbial populations in the intestinal tract is an important key to understanding the function of the gut microbiota in the digestive processes. The microbial communities of each gut region differ considerably, and the specificity of certain populations for different compartments indicates the presence of distinct ecological niches in the hindgut ecosystem. However, environmental conditions may already differ within a biofilm. For a functional analysis of the gut ecosystem, it will be necessary to elucidate the topology of the community on a microscale, the exact position of each population in the physicochemical gradients, and their mutual interactions.

ACKNOWLEDGMENTS

We thank W. Wagner (LUFA, Karlsruhe, Germany), M. Fröschle (LfP, Stuttgart, Germany), and R. Weiland (mayor of Obergrombach, Germany) for their support in the continuous supply of larvae. We are grateful to C. Schweizer (Swiss Federal Research Station for Agroecology and Agriculture, Zürich, Switzerland), R. Zelger (Research Center for Agriculture and Forestry, Laimburg, Italy), A. Reinicke (Free University of Berlin, Berlin, Germany), and S. Vestergaard (Royal Veterinary and Agricultural University, Frederiksberg, Denmark) for their kind gifts of *M. melolontha* larvae.

This study was supported by the Deutsche Forschungsgemeinschaft (DFG), the Max Planck Society, and the Fonds der Chemischen Industrie.

REFERENCES

- Amann, R. I., B. J. Binder, R. J. Olson, S. W. Chisholm, R. Devereux, and D. A. Stahl. 1990. Combination of 16S ribosomal RNA targeted oligonucleotide probes with flow cytometry for analyzing mixed microbial populations. *Appl. Environ. Microbiol.* **56**:1919–1925.
- Amann, R. I., W. Ludwig, and K. H. Schleifer. 1995. Phylogenetic identification and in-situ detection of individual microbial cells without cultivation. *Microbiol. Rev.* **59**:143–169.
- Bauchop, T., and R. T. J. Clarke. 1975. Gut microbiology and carbohydrate digestion in the larva of *Costelytra zealandica* (Coleoptera: Scarabaeidae). *N. Z. J. Zool.* **2**:237–243.
- Berchtold, M., A. Chatzinotas, W. Schönhuber, A. Brune, R. Amann, D. Hahn, and H. König. 1999. Differential enumeration and in situ localization of microorganisms in the hindgut of the lower termite *Mastotermes darwiniensis* by hybridization with rRNA-targeted probes. *Arch. Microbiol.* **172**:407–416.
- Bosshard, P. P., R. Zbinden, and M. Altwegg. 2002. *Turicibacter sanguinis* gen. nov., sp. nov., a novel anaerobic, Gram-positive bacterium. *Int. J. Syst. Evol. Microbiol.* **52**:1263–1266.
- Broderick, N. A., K. F. Raffa, R. M. Goodman, and J. Handelsman. 2004. Census of the bacterial community of the gypsy moth larval midgut by using culturing and culture-independent methods. *Appl. Environ. Microbiol.* **70**:293–300.
- Brune, A. 2003. Symbionts aiding digestion, p. 1102–1107. *In* V. H. Resh and R. T. Cardé (ed.), *Encyclopedia of insects*. Academic Press, New York, N.Y.
- Brune, A. 2005. Symbiotic associations between termites and prokaryotes. *In* *The Prokaryotes*. Springer-Verlag, New York, N.Y. [Online.] <http://141.150.157.117:8080/prokPUB/index.htm>.
- Brune, A., and M. Friedrich. 2000. Microecology of the termite gut: structure and function on a microscale. *Curr. Opin. Microbiol.* **3**:263–269.
- Cazemier, A. E., J. H. P. Hackstein, H. L. M. Op den Camp, J. Rosenberg, and C. van der Drift. 1997. Bacteria in the intestinal tract of different species of arthropods. *Microb. Ecol.* **33**:189–197.
- Charrier, M., and A. Brune. 2003. The gut microenvironment of helioid snails (Gastropoda: Pulmonata): in-situ profiles of pH, oxygen, and hydrogen determined by microsensors. *Can. J. Zool.* **81**:928–935.
- Collins, M. D., P. A. Lawson, A. Willems, J. J. Cordoba, J. Fernandez-Garayzabal, P. Garcia, J. Cai, H. Hippe, and J. A. E. Farrow. 1994. The phylogeny of the genus *Clostridium*—proposal of 5 new genera and 11 new species combinations. *Int. J. Syst. Bacteriol.* **44**:812–826.
- Crowson, R. A. 1981. *The Biology of the Coleoptera*. Academic Press, London, United Kingdom.
- Cypionka, H. 2000. Oxygen respiration by *Desulfovibrio* species. *Annu. Rev. Microbiol.* **54**:827–848.
- Daims, H., A. Brühl, R. Amann, K. H. Schleifer, and M. Wagner. 1999. The domain-specific probe EUB338 is insufficient for the detection of all *Bacteria*: development and evaluation of a more comprehensive probe set. *Syst. Appl. Microbiol.* **22**:434–444.
- Deplancke, B., K. R. Hristova, H. A. Oakley, V. J. McCracken, R. Aminov, R. I. Mackie, and H. R. Gaskins. 2000. Molecular ecological analysis of the succession and diversity of sulfate-reducing bacteria in the mouse gastrointestinal tract. *Appl. Environ. Microbiol.* **66**:2166–2174.
- Dillon, R. J., and V. M. Dillon. 2004. The gut bacteria of insects: nonpathogenic interactions. *Annu. Rev. Entomol.* **49**:71–92.
- Egert, M., and M. W. Friedrich. 2003. Formation of pseudo-terminal restriction fragments, a PCR-related bias affecting terminal restriction fragment length polymorphism analysis of microbial community structure. *Appl. Environ. Microbiol.* **69**:2555–2562.
- Egert, M., S. Marhan, B. Wagner, S. Scheu, and M. W. Friedrich. 2004. Molecular profiling of 16S rRNA genes reveals diet-related differences of microbial communities in soil, gut, and casts of *Lumbricus terrestris* L. (Oligochaeta:Lumbricidae). *FEMS Microbiol. Ecol.* **48**:187–197.
- Egert, M., B. Wagner, T. Lemke, A. Brune, and M. W. Friedrich. 2003. Microbial community structure in midgut and hindgut of the humus-feeding larva of *Pachnoda ephippiata* (Coleoptera: Scarabaeidae). *Appl. Environ. Microbiol.* **69**:6659–6668.
- Felton, G. W., and S. S. Duffey. 1991. Reassessment of the role of gut alkalinity and detergency in insect herbivory. *J. Chem. Ecol.* **17**:1821–1836.
- Friedrich, M. W. 2002. Phylogenetic analysis reveals multiple lateral transfers of adenosine-5'-phosphosulfate reductase genes among sulfate-reducing microorganisms. *J. Bacteriol.* **184**:278–289.
- Fröhlich, J., H. Sass, H. D. Babenzien, T. Kuhnigk, A. Varma, S. Saxena, C. Nalepa, P. Pfeiffer, and H. König. 1999. Isolation of *Desulfovibrio intestinalis* sp. nov. from the hindgut of the lower termite *Mastotermes darwiniensis*. *Can. J. Microbiol.* **45**:145–152.
- Grayson, J. M. 1958. Digestive tract pH of six species of *Coleoptera*. *Ann. Entomol. Soc. Am.* **51**:403–405.
- Hackstein, J. H. P., and C. K. Stumm. 1994. Methane production in terrestrial arthropods. *Proc. Natl. Acad. Sci. USA* **91**:5441–5445.
- Jackson, T. A., D. G. Boucias, and J. O. Thaler. 2001. Pathobiology of amber disease, caused by *Serratia* spp., in the New Zealand grass grub, *Costelytra zealandica*. *J. Invertebr. Pathol.* **78**:232–243.
- Kane, M. D. 1997. Microbial fermentation in insect guts, p. 231–265. *In* R. I. Mackie and B. A. White (ed.), *Gastrointestinal ecosystems and fermentations*. Chapman and Hall, New York, N.Y.
- Keller, S. 1986. *Biologie und Populationsdynamik, Historischer Rückblick, Kulturmaßnahmen. Neuere Erkenntnisse über den Maikäfer*. *Beih. Mitt. Thurgau. Naturforsch. Ges.* **1**:12–39.
- Keller, S., C. Schweizer, E. Keller, and H. Brenner. 1997. Control of white grubs (*Melolontha melolontha* L.) by treating adults with the fungus *Beauveria brongniartii*. *Biocontrol Sci. Technol.* **7**:105–116.
- Klein, M. G., and T. A. Jackson. 1992. Bacterial diseases of scarabs, p. 43–61. *In* T. R. Glare and T. A. Jackson (ed.), *Use of pathogens in scarab pest management*. Intercept Ltd., Andover, United Kingdom.
- Kuhnigk, T., J. Branke, D. Krekeler, H. Cypionka, and H. König. 1996. A feasible role of sulfate-reducing bacteria in the termite gut. *Syst. Appl. Microbiol.* **19**:139–149.
- Lemke, T., U. Stingl, M. Egert, M. W. Friedrich, and A. Brune. 2003. Physicochemical conditions and microbial activities in the highly alkaline gut of the humus-feeding larva of *Pachnoda ephippiata* (Coleoptera: Scarabaeidae). *Appl. Environ. Microbiol.* **69**:6650–6658.
- Li, X., and A. Brune. 2005. Digestion of microbial biomass, structural polysaccharides, and protein by the humivorous larva of *Pachnoda ephippiata* (Coleoptera: Scarabaeidae). *Soil Biol. Biochem.* **37**:107–116.
- Loubinoux, J., F. Mory, I. A. C. Pereira, and A. E. Le Faou. 2000. Bacteremia caused by a strain of *Desulfovibrio* related to the provisionally named *Desulfovibrio fairfieldensis*. *J. Clin. Microbiol.* **38**:931–934.
- Manz, W., M. Eisenbrecher, T. R. Neu, and U. Szewzyk. 1998. Abundance and spatial organization of Gram-negative sulfate-reducing bacteria in activated sludge investigated by in situ probing with specific 16S rRNA targeted oligonucleotides. *FEMS Microbiol. Ecol.* **25**:43–61.
- Martin, J. S., M. M. Martin, and E. A. Bernays. 1987. Failure of tannic acid

- to inhibit digestion or reduce digestibility of plant protein in gut fluids of insect herbivores—implications for theories of plant defense. *J. Chem. Ecol.* **13**:605–621.
37. Muzyer, G., A. Teske, C. O. Wirsén, and H. W. Jannasch. 1995. Phylogenetic relationships of *Thiomicrospira* species and their identification in deep-sea hydrothermal vent samples by denaturing gradient gel-electrophoresis of 16S rDNA fragments. *Arch. Microbiol.* **164**:165–172.
 38. Pernthaler, J., F. O. Glöckner, W. Schönhuber, and R. Amann. 2001. Fluorescence in situ hybridization (FISH) with rRNA-targeted oligonucleotide probes. *Methods Microbiol.* **30**:207–226.
 39. Potter, D. A., and D. W. Held. 2002. Biology and management of the Japanese beetle. *Annu. Rev. Entomol.* **47**:175–205.
 40. Raskin, L., J. M. Stromley, B. E. Rittmann, and D. A. Stahl. 1994. Group-specific 16S ribosomal-RNA hybridization probes to describe natural communities of methanogens. *Appl. Environ. Microbiol.* **60**:1232–1240.
 41. Rössler, M. E. 1961. Ernährungsphysiologische Untersuchungen an Scarabaeidenlarven (*Oryctes nasicornis* L., *Melolontha melolontha* L.). *J. Insect Physiol.* **6**:62–80.
 42. Sass, H., M. Berchtold, J. Branke, H. König, H. Cypionka, and H. D. Babenzien. 1998. Psychrotolerant sulfate-reducing bacteria from an oxic freshwater sediment, description of *Desulfovibrio cuneatus* sp. nov. and *Desulfovibrio litoralis* sp. nov. *Syst. Appl. Microbiol.* **21**:212–219.
 43. Schmitt-Wagner, D., and A. Brune. 1999. Hydrogen profiles and localization of methanogenic activities in the highly compartmentalized hindgut of soil-feeding higher termites (*Cubitermes* spp.). *Appl. Environ. Microbiol.* **65**:4490–4496.
 44. Shah, P. A., and J. K. Pell. 2003. Entomopathogenic fungi as biological control agents. *Appl. Microbiol. Biotechnol.* **61**:413–423.
 45. Stackebrandt, E., and B. M. Goebel. 1994. A place for DNA-DNA reassociation and 16S ribosomal-RNA sequence-analysis in the present species definition in bacteriology. *Int. J. Syst. Bacteriol.* **44**:846–849.
 46. Stahl, D. A., and R. Amann. 1991. Development and application of nucleic acid probes, p. 205–248. In E. Stackebrandt and M. Goodfellow (ed.), *Nucleic acid techniques in bacterial systematics*. John Wiley & Sons Ltd., Chichester, England.
 47. Terra, W. R., and C. Ferreira. 1994. Insect digestive enzymes—properties, compartmentalization and function. *Comp. Biochem. Physiol. B* **109**:1–62.
 48. Tholen, A., and A. Brune. 2000. Impact of oxygen on metabolic fluxes and in situ rates of reductive acetogenesis in the hindgut of the wood-feeding termite *Reticulitermes flavipes*. *Environ. Microbiol.* **2**:436–449.
 49. Tholen, A., B. Schink, and A. Brune. 1997. The gut microflora of *Reticulitermes flavipes*, its relation to oxygen, and evidence for oxygen-dependent acetogenesis by the most abundant *Enterococcus* sp. *FEMS Microbiol. Ecol.* **24**:137–149.
 50. Trinkerl, M., A. Breunig, R. Schauder, and H. König. 1990. *Desulfovibrio termitidis* sp. nov., a carbohydrate degrading sulfate-reducing bacterium from the hindgut of a termite. *Syst. Appl. Microbiol.* **13**:372–377.
 51. von Wintzingerode, F., U. B. Göbel, and E. Stackebrandt. 1997. Determination of microbial diversity in environmental samples: pitfalls of PCR-based rRNA analysis. *FEMS Microbiol. Rev.* **21**:213–229.
 52. Werner, E. 1928. Der Erreger der Zelluloseverdauung bei der Rosenkäferlarve, *Bacillus cellulosam fermentans*. *Zentbl. Bakteriologie II* **67**:297–330.
 53. Wiedemann, J. F. 1930. Die Zelluloseverdauung bei Lamellicornierlarven. *Z. Morph. Ökol. Tiere.* **19**:228–258.
 54. Wildbolz, T. 1954. Beitrag zur Anatomie, Histologie und Physiologie des Darmkanals der Larve von *Melolontha melolontha* L. *Mitt. Schweizerischen Entomol. Gesellschaft* **27**:193–239.
 55. Wolters, V. 2000. Invertebrate control of soil organic matter stability. *Biol. Fertil. Soils* **31**:1–19.
 56. Yang, H., D. Schmitt-Wagner, U. Stingl, and A. Brune. 2005. Niche heterogeneity determines bacterial community structure in the termite gut (*Reticulitermes santonensis*). *Environ. Microbiol.* **7**:916–932.